BioShield-12: A Wearable 12-Lead ECG based Chest Shield with IoT Integrated Diagnostic system

Abstract — cardiovascular diseases (CVDs) are the principal cause of death worldwide, claiming 17.9 million lives a year, according to the World Health Organization (WHO). Early diagnosis and constant monitoring is important for timely intervention, as well as better patient outcome. Among methods of non-invasive diagnostics, electrocardiography (ECG) is one of the best tools for determination of cardiac abnormalities such as ischemia, conduction disorders and arrhythmias by waveform morphologies analysis. The clinical gold standard for ECG measurement is the 12-lead system; however, traditional setups for ECG measurements in hospitals are often bulky, wired, and very dependent on operator expertise. These limitations limit their application in prehospital, remote or emergency care situations. To fix these issues, a number of recent studies have been conducted on wearable and wireless electrocardiogram (ECG) technologies to offer mobility and real-time monitoring. While these designs show promising results, many of them suffer from limited lead coverage, less comfort and unstable wireless communication, which makes the diagnostic reliability questionable. To address these limitations, this paper introduces BioShield-12, a low-power, 12-lead wearable ECG system that is able to perform continuous real-time cardiac monitoring. The device has a flexible Thermoplastic Polyurethane (TPU) shield which preserves the electrode geometry while conforming to the skin surface. TPU was chosen by material characterization in the PASCO Capstone materials testing machine due to its high tensile strength and elasticity. BioShield-12 allows high-quality data acquisition and dependable (wireless) data transmission for both clinical and remote diagnostics. Future work will focus on integrating cloud-based data management with multi-user connectivity for broader use in community health and emergency response systems.

keywords—wearable ECG, 12-lead ECG, morphological analysis, wireless transmission, portable monitoring.

I. INTRODUCTION

The main cause of mortality in the world has remained cardiovascular diseases (CVDs), as it is estimated that almost 17.9 million deaths per year occur due to these diseases (World Health Organization, WHO). Such diseases are coronary artery disease, myocardial infarction, and arrhythmias, which alone create a significant health and economic burden in the world. Timely intervention and better patient outcome depend on early diagnosis and constant observation. The electrocardiogram (ECG) has been the most efficient, non-invasive, and available mode of measuring the cardiac electrophysiological activity. It allows clinicians to detect abnormalities like ischemia, conduction disorders and arrhythmias using the morphology of P waves, QRS complexes and T waves. The clinical cardiac assessment gold standard is the 12-lead ECG pattern that offers spatially distributed cardiac vectors of ten electrodes.

Traditional 12-lead ECG systems are, however, mostly confined to the controlled hospital environment because the system has a wired format, requires the use of a trained operator to place the electrodes and is not portable. These systems do not support continuous ambulatory monitoring or fast prehospital evaluation especially in resource constrained or remote locations. The additional factors that affect signal quality in a mobile scenario are motion artifact, electromagnetic interference, and the electrode-skin impedance change, which result in the possibility of misinterpreting cardiac events that are important. This leads to the growing need of portable, inexpensive, and easy to use ECG devices that can deliver the quality of diagnostic results offered by a hospital without necessarily being in a clinical environment.

The past years have seen innovations in wearable electronics and biomedical signal acquisition which have led to the creation of portable and wireless ECG monitoring systems. Scholars have explored flexible electrode, cloth-based sensor, and microcontroller-based telemetry in order to accomplish real-time cardiac signal recording. Still, full 12-lead functionality in a wearable format is still technically difficult due to the fact that it needs proper placement of electrodes, simultaneous acquisition of multi-channels, and reliability of wireless data transmission without major signal impairment. Also, a majority of commercial portable ECG systems have a maximum of 1-3 leads and this limits its diagnostic application in relation to the conventional 12-lead systems.

Recent researchers have worked on enhancing the use of multi-lead cardiac monitoring using portable and wireless systems. Jo et al. (2021) tested a handheld 12-lead ECG device, which has proven to be accurate in its diagnosis and easy to use. The device however necessitated manual placement of electrodes and was primarily tested in a stationary situation and was not that applicable to an ambulatory or the continuous use. The Park et al. (2020) introduced a wearable wireless ECG monitoring system that consumed a low power, but the design was reduced to the lesser number of leads and it failed to support 12-leads. Equally, Borde et al. (2024) introduced a 12-lead ECG device with a Bluetooth connection, which demonstrated good diagnostic accuracy in the clinical setting. Nevertheless, it was based on temporary Bluetooth communications and was not integrated with bigger data transmission systems, which decreased its applicability to remote

monitoring in real time. In general, these studies show that there has been advancement in portable ECG technology but most of the current systems have become constrained in lead coverage, range of communication and the life of material.

This paper presents BioShield-12, a wearable 12-lead ECG system designed to achieve low power consumption and high signal fidelity. The device features a flexible thermoplastic polyurethane (TPU) shield that ensures stable electrode geometry, user comfort, and mechanical durability. Material evaluation conducted using the PASCO Capstone testing system identified TPU as the optimal choice due to its superior tensile strength and elasticity. With integrated wireless transmission and high-resolution data acquisition, BioShield-12 enables reliable real-time cardiac monitoring in both clinical and remote environments.

II. METHODOLOGY:

The BioShield-12 system architecture is described in Figure 1. Eleven chest electrodes are placed as shown in Figure 1a and interfaced with a flexible shield of thermoplastic polyurethane (TPU) (Figure 1b), which ensures secure contact and electrode geometry. The shield combines routing channels and circuitry housing (Figure 1c) for amplification, filtering, digitization and power management (Figure 1a), The processed signals are then sent via a wireless link to a MATLAB interface to be displayed and stored in real time (Figure 1d). This configuration allows for more compact, low noisy and reliable ECG simultaneous multi-lead monitoring.

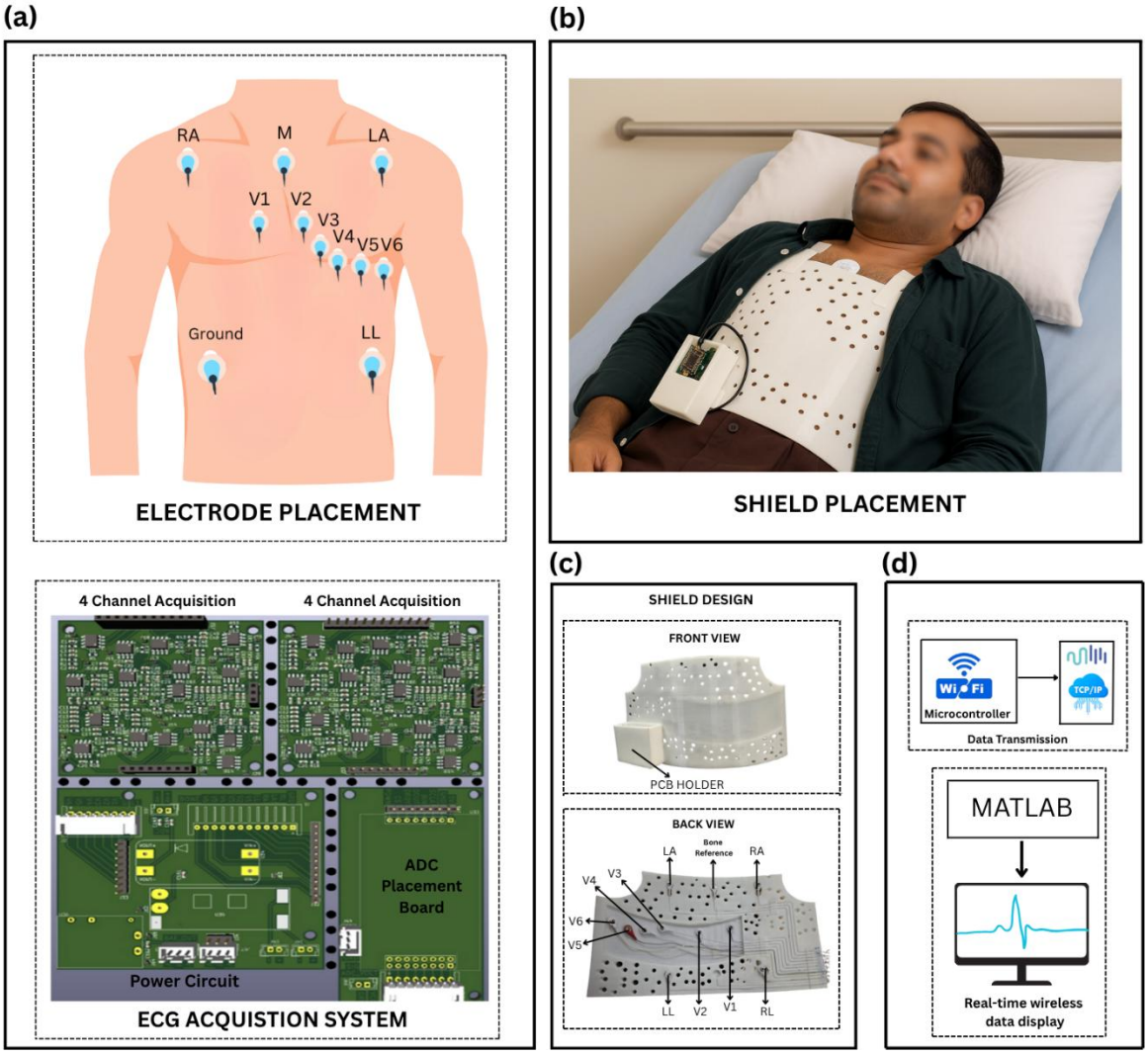

Figure 1 depicts the overall technique for the designed 12-lead ECG acquisition system, from signal acquisition to wireless data presentation. In (a), electrodes placement using the usual 12-lead ECG placement, ensuring accurate cardiac potential measurement is shown, while the custom-designed ECG acquisition system is depicted, which includes two 4-channel acquisition modules that are interfaced with an ADC placement board and a power circuit. (b) a wearable shield incorporated with electrode connectors ensures secure and constant placement during recording. The shield design in (c) shows both front and back views of how electrodes and the PCB holder are integrated to preserve solid contact and reduce noise interference during measurement. Finally, as shown in (d), the recorded ECG signals are wirelessly transferred to MATLAB via a Wi-Fi-enabled microcontroller, where they are processed and shown in real time for analysis.

A. SHIELD DESIGN FOR WEARABLE ECG ACQUISITION

The shape design of the wearable BioShield-12 was made by creating a chest shield that was 3D-printed and had electrode embedded channels made on it in the proper position relative to the anatomical landmarks required to accurately record 12-lead ECGs. The shield was made of flexible thermoplastic polyurethane (TPU) material to ensure maximum skin contact, comfort, and strength in applications of prolonged wearing. Also, the shield was designed with a special mounting area to allow safe mounting of the signal acquisition circuitry making the design very compact and ergonomically stable that can be adapted to the clinical and ambulatory setting.

1) Mechanical Design and Integration Framework

Mechanical and spatial calculations were made and carefully considered in the BioShield-12 in order to achieve correct positioning of electrodes and steady operation. The shield is about 12.5 inches by 17 inches, and is curved along the normal thoracic curve to make the most contact. The PCB holder (12x 10x 2 cm) is placed at the front to encapsulate the circuitry for signal acquisition. Embedded routing channels fix electrode wires, eliminating motion artifact and providing constant signal paths.

2) Shield Design Based on Thoracic Anatomy

The BioShield-12 has a geometrical design based on detailed analysis of adult thoracic anatomy, to achieve physiologically correct lead in standard position and improved user comfort when worn over long periods of time. The shield is equipped with custom ECG channels located with anatomic guided channels matching the standard precordial lead locations (V1-V6) in the fifth intercostal space assuring all electrode spacing is constant and vectors are recorded accurately. The type of electrode placed nearby the manubrium sterni gives a steady ground level for unipolar measurements. In order to reduce the wiring complexity and to maximize the mobility, the limb equivalent leads (RA, LA, LL) are located on the upper torso.

3) Material Evaluation and Selection

In order to evaluate the mechanical behavior of materials for the BioShield-12 shield, tensile tests were performed with PASCO Materials Testing Machine (Model ME-8236) fitted with 7,100 N load cell and optical encoder to measure the displacement. Standardized gauge lengths and cross-sectional areas of thermoplastic polyurethane (TPU), acrylonitrile butadiene styrene (ABS) and flexible resin were prepared. The specimens were placed in the machine grips and uniaxial tension loading was applied at a constant speed of cross head until failure. Force and displacement were continuously recorded using PASCO Capstone software and corresponding stress-strain curves were obtained to provide parameters such as toughness, ultimate tensile strength, and Young's modulus.

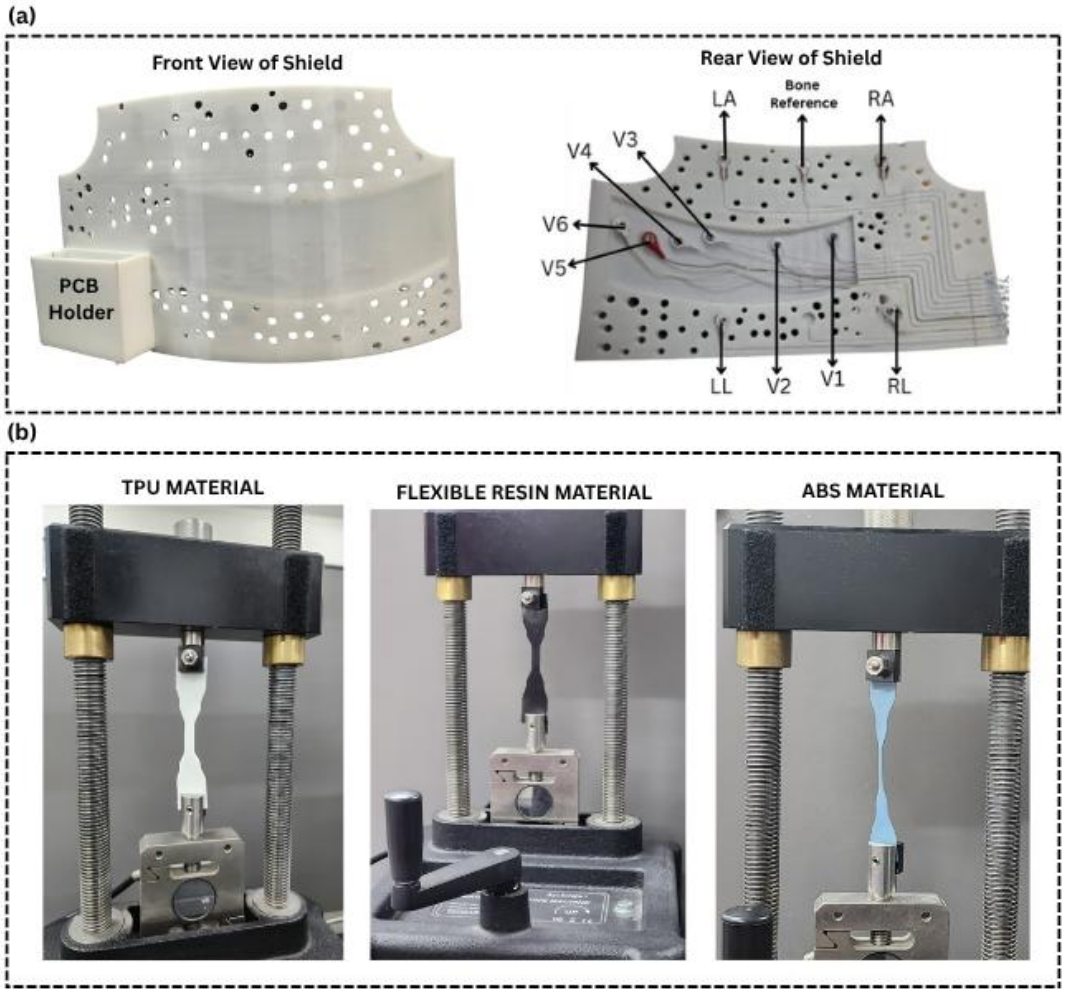

Figure 5 1 (a) depicts the overall 3D printed design of the chest shield with the correct anatomical positions of the chest and limb leads while Figure 5(b) depicts the testing of three different materials in PASCO Testing Machine to select the best material for the chest shield.

A. Analog Front-End and Signal Acquisition

The analog front-end was developed to preserve the integrity of low-amplitude ECG biopotentials and ensure clean signal acquisition. The circuit layout followed a signal-flow approach, with each stage arranged sequentially, including input protection, amplification, filtering, and buffering, to minimize high-impedance trace lengths. Each acquisition board incorporated a continuous ground plane with a centralized star-ground node to eliminate loops and maintain a stable reference. Guard rings were placed around the INA129 amplifier inputs to prevent leakage currents, while differential routing between the acquisition stage and ADC improved common-mode noise rejection. Component selection focused on precision and low noise. The INA129 instrumentation amplifier provided a gain of 8, while high-pass (0.1 Hz) and low-pass (100 Hz) Bessel filters, implemented in the Sallen-Key topology, ensured a linear phase response within the diagnostic ECG bandwidth. The 24-bit ADS1256 ADC was used for digitization, offering a resolution of 0.298 μV per LSB, which allowed accurate detection of subtle ECG waveform features.

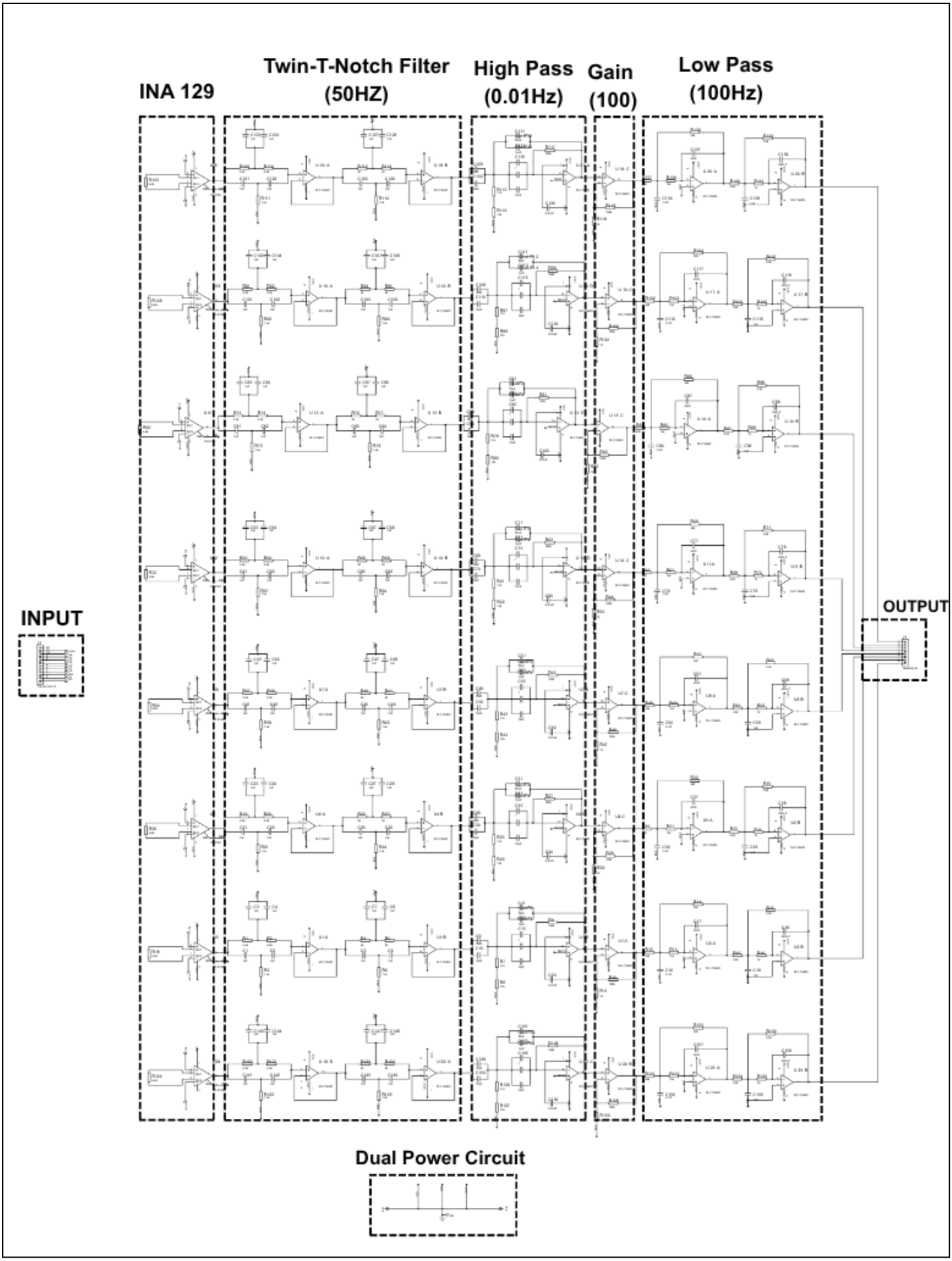
INA 129
Twin-T-Notch Filter
(50HZ)
High Pass
(0.01Hz)
Gain
(100)
Low Pass
(100Hz)
INPUT
OUTPUT
Dual Power Circuit

B. PCB DESIGNING OF ECG ACQUISITION SYSTEM

The PCB design of the BioShield-12 was a key engineering step that converted the analog front-end and system layout into a working hardware prototype. The main goals were to maintain the ECG signal's microvolt-level accuracy, keep the design compact and wearable, and ensure stable performance in noisy environments. These goals were achieved using a modular, stacked PCB design that separates each function to reduce interference and improve reliability.

1) Stacked PCB Design

To manage system complexity and minimize interference between analog and digital sections, a four-board stacked PCB architecture was implemented, as shown in Figure 2. The setup includes two identical 6×6 cm ECG acquisition boards, each handling four channels to collectively cover all twelve ECG leads. Each of these boards functions as an independent analog signal conditioning unit. A 7×7.8 cm power management board utilized a 2-cell lithium-ion battery pack equipped with a 2S Battery Management System (HX-2S-JH10) for safe charging, over-discharge, and short-circuit protection. Regulated supply rails were generated through an MT3608 DC-DC boost converter, providing ±3.7 V for analog circuitry and 5 V for digital components. A dedicated reference voltage (REF) was distributed across acquisition boards to maintain consistent biasing and signal stability. generates stable, low-noise supply rails (±3.7 V for analog and 5 V for digital) from a two-cell Li-ion battery, with integrated protection and regulation circuits. The 4.3×8.4 cm ADC and communication board serves as the digital hub, integrating the ADS1256 high-resolution ADC and ESP32-S3 microcontroller for signal digitization, processing, and wireless data transmission between the analog and digital domains.

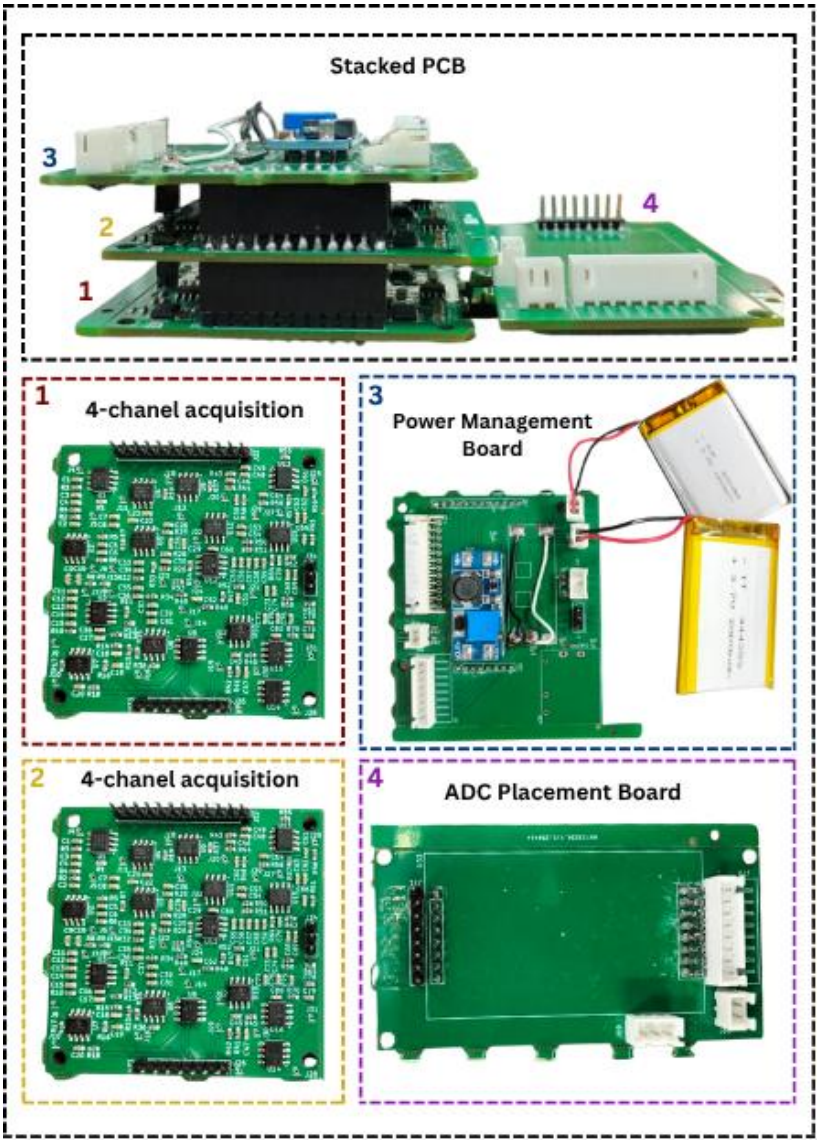

Figure 2: A stacked PCB structure that has four parts i.e. at top power management and I/O attachments for ECG Leads, bottom two are 4 channel ECG acquisition boards and last we have the ADC attachment board along with esp32 for data conversion,processing and wireless transmission

C. LEAD FORMATION AND SIGNAL DERIVATION IN 12-LEAD ECG

The BioShield-12 system implements a specialized lead formation strategy that utilizes direct unipolar precordial measurements referenced to the manubrium, combined with mathematically derived limb leads. This approach eliminates the need for a traditional Wilson Central Terminal (WCT) while maintaining full 12-lead signal integrity.

1) ECG Lead Acquisition Framework

The BioShield-12 system employs a modified 12-lead acquisition framework that integrates unipolar precordial and bipolar limb configurations. All precordial potentials (V1–V6) are recorded as differential measurements between the respective chest electrodes and a stable manubrium reference, expressed as $V_n = Chest_{Vn} - Manubrium_{Ref}$. This method eliminates the conventional Wilson Central Terminal while maintaining accurate representation of horizontal plane cardiac activity. Limb electrodes, repositioned on the upper torso for improved wearability, are used to compute the standard bipolar and augmented leads based on established Einthoven and Goldberger relationships. The anatomical placement of the precordial electrodes follows standard clinical conventions, extending from the right sternal border (V1) to the midaxillary line (V6), thereby ensuring reliable spatial mapping of ventricular depolarization and repolarization dynamics.

Mathematical Formulas for Limb and Chest Leads	
LEAD	**FORMULA**
LEAD II	LEAD II = LEAD I + LEAD III
aVR	$\frac{RA - (LA + LL)}{2}$
aVL	$\frac{LA - (RA + LL)}{2}$
aVF	$\frac{LL - (RA + LA)}{2}$
V1	$Chest_{V1} - Manubrium_{Ref}$
V2	$Chest_{V2} - Manubrium_{Ref}$
V3	$Chest_{V3} - Manubrium_{Ref}$
V4	$Chest_{V4} - Manubrium_{Ref}$

V5	$Chest_{V5} - Manubrium_{Ref}$
V6	$Chest_{V6} - Manubrium_{Ref}$

Table 1 Lead Calculation Formulas

2) Signal Processing

The system first acquires raw signals from 8 channels using the ESP32-S3 microcontroller. These signals are then digitally processed on the microcontroller, where filtering and augmentation steps are applied to remove DC offsets and high-frequency noise. Subsequently, the processed signals are used to compute additional leads according to standard lead derivation formulas, allowing the derivation of a complete 12-lead ECG from the original 8 acquired channels. This approach ensures that the 12-lead signals are consistently generated in real time, with fixed electrode positions maintained by the custom shield design to guarantee reproducible results across multiple recordings and operators.

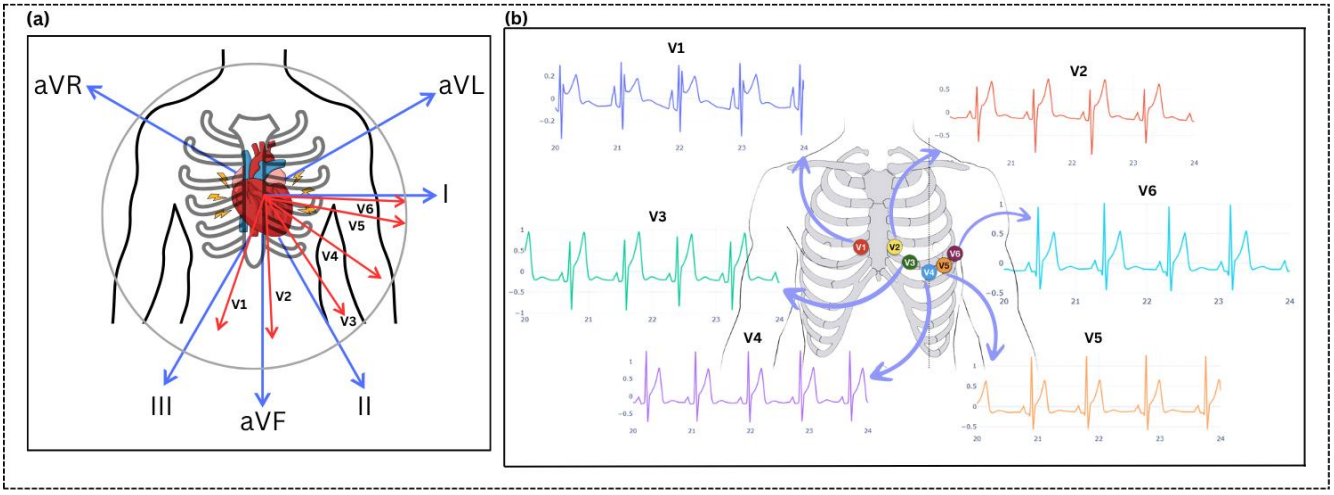

*Figure 4 (a) shows the 12-lead ECG orientations, illustrating how limb leads (blue) and chest leads (red) record the heart's electrical activity from different angles. It represents both the **frontal and horizontal planes** of cardiac electrical monitoring. (b) shows the waveforms obtained by acquiring signals from chest leads (V1-V6).*

D. Comparative Analysis of ECG Acquisition

The performance of the BioShield-12 system was assessed through a structured evaluation protocol to verify signal accuracy and reliability. Validation was conducted in two stages: comparative testing with research-grade equipment and verification using standardized ECG simulation. In the first stage, the BioShield-12 system was directly compared with the BIOPAC MP36, which served as the reference standard. Simultaneous ECG recordings were obtained from healthy adult participant using identical electrode placements based on standard clinical positions. Participant remained in a resting supine posture to minimize motion artifacts, and data were acquired for at least one minute to ensure sufficient cardiac cycles for analysis. In the second stage,

a SEG-A ECG Simulator provided calibrated reference signals, enabling precise assessment of the system's amplitude accuracy and waveform fidelity relative to known inputs. This validation framework confirmed the BioShield-12's capability to produce consistent, high-fidelity ECG data suitable for diagnostic and research applications.

1) **Quantitative Signal Quality Assessment**

Signal quality was evaluated using multiple quantitative metrics to assess the reliability of the acquired ECG signals, as illustrated in Figure 5. The signal-to-noise ratio (SNR) was used to quantify the effectiveness of the analog front-end and filtering stages in preserving physiological signal components while minimizing powerline and environmental interference. Pearson correlation coefficients were calculated to determine morphological similarity between BioShield-12 and reference recordings, ensuring preservation of key diagnostic features such as the P-wave, QRS complex, and ST segment. In addition, higher-order statistical parameters, including kurtosis and skewness, were analyzed to identify subtle waveform distortions and non-Gaussian noise components that could influence automated analysis or clinical interpretation.

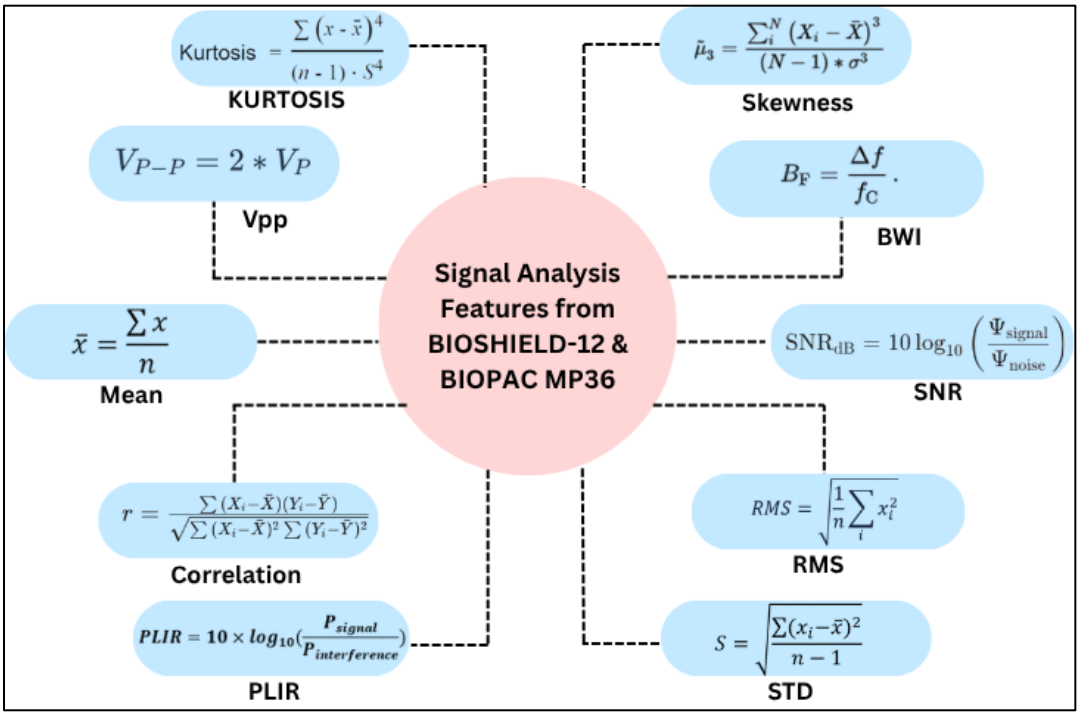

Figure 5: the signals acquired from our system BIOSHIELD-12 were compared with the same signals acquired from a research grade equipment BIOPAC MP36 by using MATLAB to calculate relevant metrices for comparative analysis

E. WIRELESS DATA STREAMING AND IoT INTEGRATION

The BioShield-12 system implements a sophisticated wireless communication framework that enables real-time ECG data transmission and visualization through a coordinated hardware-software architecture.

1) Wireless Communication Architecture

The BioShield-12 system incorporates a wireless communication framework that enables real-time ECG data transmission and visualization. The architecture follows a client–server model using the TCP/IP protocol, where the ESP32-S3 microcontroller acts as a self-contained web server and MATLAB functions as the client interface. The ESP32 establishes a secure wireless access point, creating an isolated local network to prevent interference and ensure data security. ECG signals acquired through the ADS1256 ADC at a 1000 Hz sampling rate are processed by the ESP32, which converts raw ADC readings to voltage values, removes DC bias, and buffers samples for efficient transmission. Upon receiving HTTP GET requests from MATLAB, the server transmits the data in comma-separated format using a non-blocking communication routine, ensuring uninterrupted sampling and minimal latency.

2) Real-Time Data Reception and Visualization

On the client side, MATLAB maintains a persistent TCP connection with the ESP32 server to receive ECG data streams in real time. The acquired data are parsed into numerical arrays, validated for transmission integrity, and continuously plotted for live visualization. The display dynamically adjusts axes and scaling to highlight diagnostic waveform features, including P-waves, QRS complexes, and T-waves. To maintain synchronization between acquisition and display, the ESP32 employs precise timing control using microsecond-level delays, while MATLAB regulates refresh intervals for smooth visualization. The communication framework includes compression and automatic reconnection routines to ensure continuous operation during transient network disruptions. As demonstrated in Figure 7, the implemented architecture reliably

delivers diagnostic-quality ECG signals with low latency, validating its suitability for portable and remote cardiac monitoring applications.

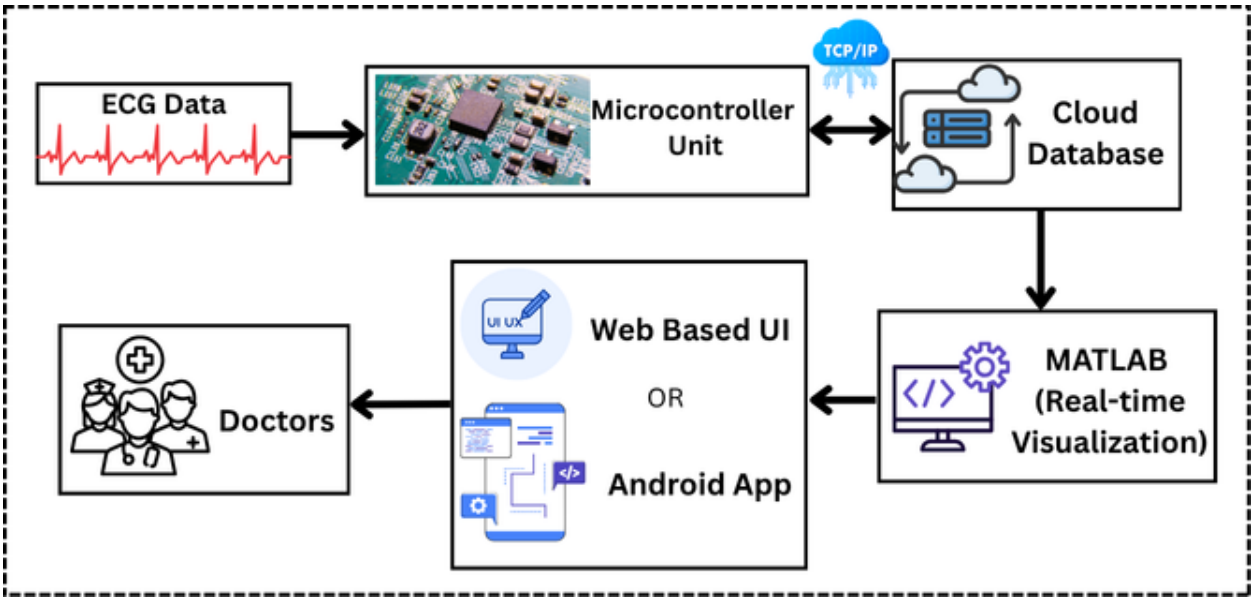

Figure 7: The flow chart for ECG data being fed to microcontroller for processing and wireless transmission to MATLAB to visualize in real-time.

III. RESULTS:

This section presents the experimental validation of the BioShield-12 system, focusing on material performance and signal acquisition quality. The results demonstrate the system's capability to reliably acquire diagnostic-grade ECG signals while maintaining structural integrity and user comfort.

1) Mechanical and Material Performance of TPU Shield

The comparative evaluation of mechanical performance for ABS, Flexible Resin, and TPU materials provides critical insights into their suitability for the BioShield-12 system's protective architecture. Among the tested materials, TPU demonstrated exceptionally high toughness (34,426.99 MJ/m³), indicating superior energy absorption capacity and excellent deformation tolerance under applied stress. Its ultimate tensile strength (UTS) of 40,061.99 MPa and Young's modulus of 79.06 GPa confirm remarkable strength and flexibility, making it ideal for BioShield-

12 components that require both impact resistance and structural adaptability. Flexible Resin, with a toughness of 164.85 MJ/m³, UTS of 2,577.60 MPa, and modulus of 45.25 GPa, exhibited a moderate balance between stiffness and elasticity, representing intermediate mechanical performance. In contrast, ABS showed the lowest mechanical resilience, with a toughness of 36.15 MJ/m³, UTS of 187.17 MPa, and modulus of 3.14 GPa, reflecting a brittle nature and limited ability to sustain mechanical deformation. Collectively, these findings validate the selection of TPU as the optimal material for the BioShield-12's outer protective structure, ensuring high durability, flexibility, and impact absorption while maintaining ergonomic comfort and design reliability.

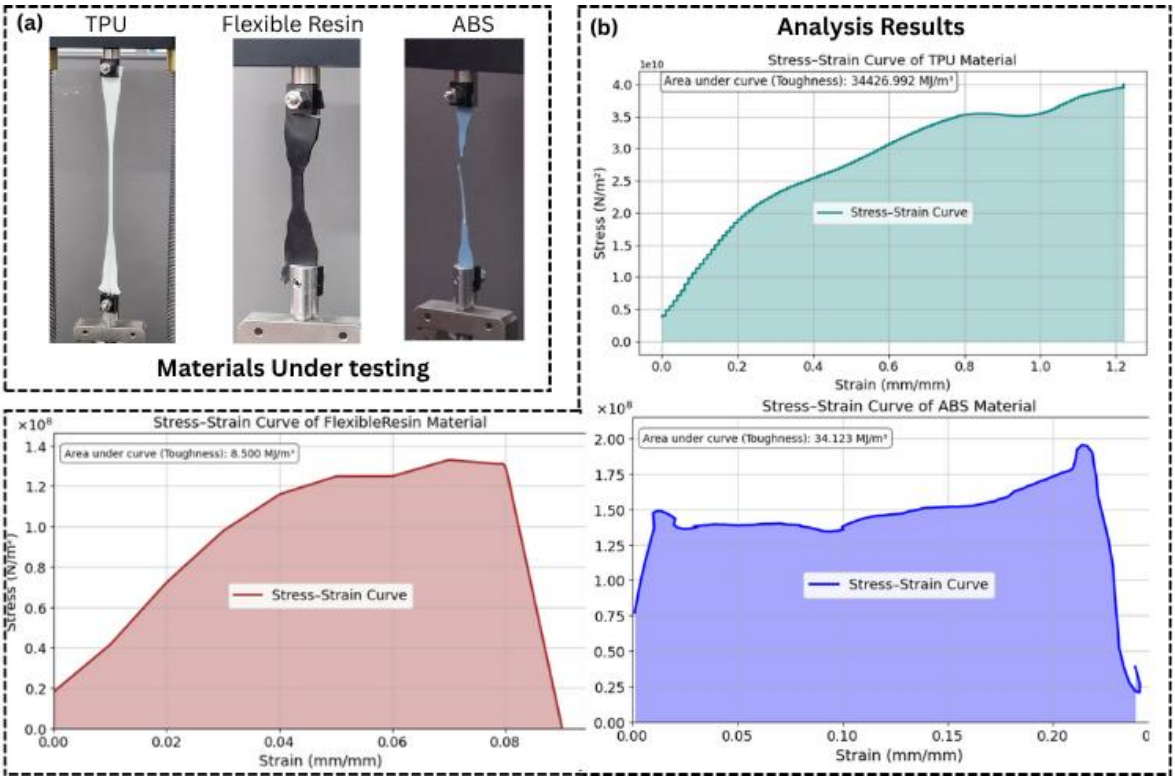

2) Signal Quality Evaluation

2.1.1 Human Subject Signal Analysis

Quantitative analysis of ECG signals acquired from human subjects demonstrated excellent performance of the BioShield-12 acquisition system. As summarized in Table 4, the system achieved an average Signal-to-Noise Ratio (SNR) of 23.8 ± 1.6 dB across all twelve leads, confirming strong noise immunity and signal fidelity. Among the precordial leads, V3–V6 exhibited the highest SNR values (25.2 ± 1.1 dB), while the limb leads maintained 22.4 ± 1.3 dB, indicating consistent performance across different electrode placements. These results highlight the system's ability to maintain diagnostic-grade ECG quality during real-time human recordings while effectively suppressing motion and baseline interference.

2.1.2 Comparative Validation with BIOPAC System

The designed ECG acquisition circuit was rigorously benchmarked against a BIOPAC research-grade system using both simulator-generated and in-vivo ECG signals. Comparative evaluation across the standard 12-lead configuration employed a comprehensive set of quantitative metrics, including SNR, skewness, kurtosis, mean, standard deviation (Std), root-mean-square (RMS), peak-to-peak amplitude (PtP), Bandwidth Index (BWI), and Power Line Interference Ratio (PLIR). The results, summarized in Tables 2 and 3, confirm that the BioShield-12 circuit achieves measurement accuracy and consistency closely matching BIOPAC. The circuit's gain of 800, deliberately implemented to enhance the low-amplitude millivolt ECG signals into a more robust processing range, ensures improved resolution and signal clarity without compromising waveform morphology or frequency content.

2.1.3 Simulator-Based Performance Assessment

In simulator-based testing, the BioShield-12 circuit achieved SNR values between 14.17–19.40 dB for the precordial leads (V1–V6) and up to 31.11 dB for Lead I, closely comparable to BIOPAC, which reported ~19.69 dB across chest leads and 32.97 dB for Lead I. Minor deviations observed in lower chest leads (V3–V4) are attributed to inherent simulator modeling and lead-placement variability rather than circuit performance.

Amplitude-related metrics confirmed the intended amplification behavior: RMS values up to 16.5 mV (V6) from the BioShield-12 correspond to amplified forms of baseline simulator signals, while BIOPAC recorded ~1.02 mV under its default gain. This proportionality across all leads verifies uniform gain application and distortion-free amplification.

Statistical features further validate signal fidelity — the circuit produced skewness values between 0.6–0.8 for chest leads (versus BIOPAC's –0.9 to –1.0), with polarity differences arising from reference alignment rather than waveform degradation. Kurtosis values of 3.9–4.2 align with physiologically expected QRS peakedness, while BIOPAC's higher (16–20) values reflect sharper peak sensitivity. Both systems exhibited negligible PLIR ($\sim 10^{-5}$), confirming effective 50/60 Hz noise rejection, and BWI values of 0.03–0.04 (BioShield-12) versus 0.44–0.52 (BIOPAC), indicating minor spectral variation consistent with amplified scaling but well within diagnostic tolerance.

Signal Acquired from simulator through Biopac	SNR	Skewness	Kurtosis	Mean	Std	RMS	Ptp	BWI	PLIR
V6	19.69	-0.97	20.80	-0.9980	0.1968	1.0173	3.8097	0.51971	0.00001
V5	19.69	-1.01	17.78	-0.9978	0.2266	1.0232	4.0730	0.46400	0.00001
V4	19.69	-1.04	16.27	-0.9975	0.2545	1.0295	4.3285	0.44106	0.00002
V3	19.69	-1.07	16.21	-0.9974	0.2668	1.0324	4.4472	0.41597	0.00002
Lead I	32.97	3.63	15.60	0	0.2130	0.2130	1.1770	0.02298	0.00002
Lead II	7.08	0.57	12.10	0	0.1453	0.1453	1.7354	0.43825	0.00002
Lead III	3.81	-3.01	29.70	0	0.0997	0.0997	1.2820	0.63972	0.00002
aVR	10.99	-2.47	12.10	0	0.1902	0.1902	1.8354	0.27951	0.00002
aVF	4.99	-2.46	13.51	0	0.1143	0.1143	1.5035	0.55768	0.00002
aVL	6.52	-1.44	18.78	0	0.1369	0.1369	1.3103	0.46742	0.00002

Table 2: Comparative Metrices of the Signal Acquired from simulator through BIOPAC

2.1.4 Visual Comparison

To supplement numerical evaluation, **waveform overlays** between the circuit and BIOPAC signals were generated as shown in figure 8. Simulator-based ECG plots show excellent temporal alignment and morphology preservation, particularly in the P–QRS–T segments. The **R-wave peak amplitudes** scale proportionally, and baseline stability is evident across all leads.

Figure 8: Simulator-based comparison showing 3 out of 12 signals that are being visually compared. The signals were taken from our system first and then same signals from BIOPAC also depicting comparable results.

2.1.5 Spectral (FFT and PSD) Analysis

The **Fast Fourier Transform (FFT)** and **Power Spectral Density (PSD)** plots as depicted in figure 9 further confirms spectral similarity between the two systems.

- Both spectra exhibit dominant power below **40 Hz**, typical for ECG signals.
- The circuit's FFT displays slightly higher magnitude due to the designed amplification, but spectral shape and frequency content remain consistent.

- PSD plots highlight identical power concentration in low-frequency bands (0.5–40 Hz), verifying no artificial frequency components were introduced.

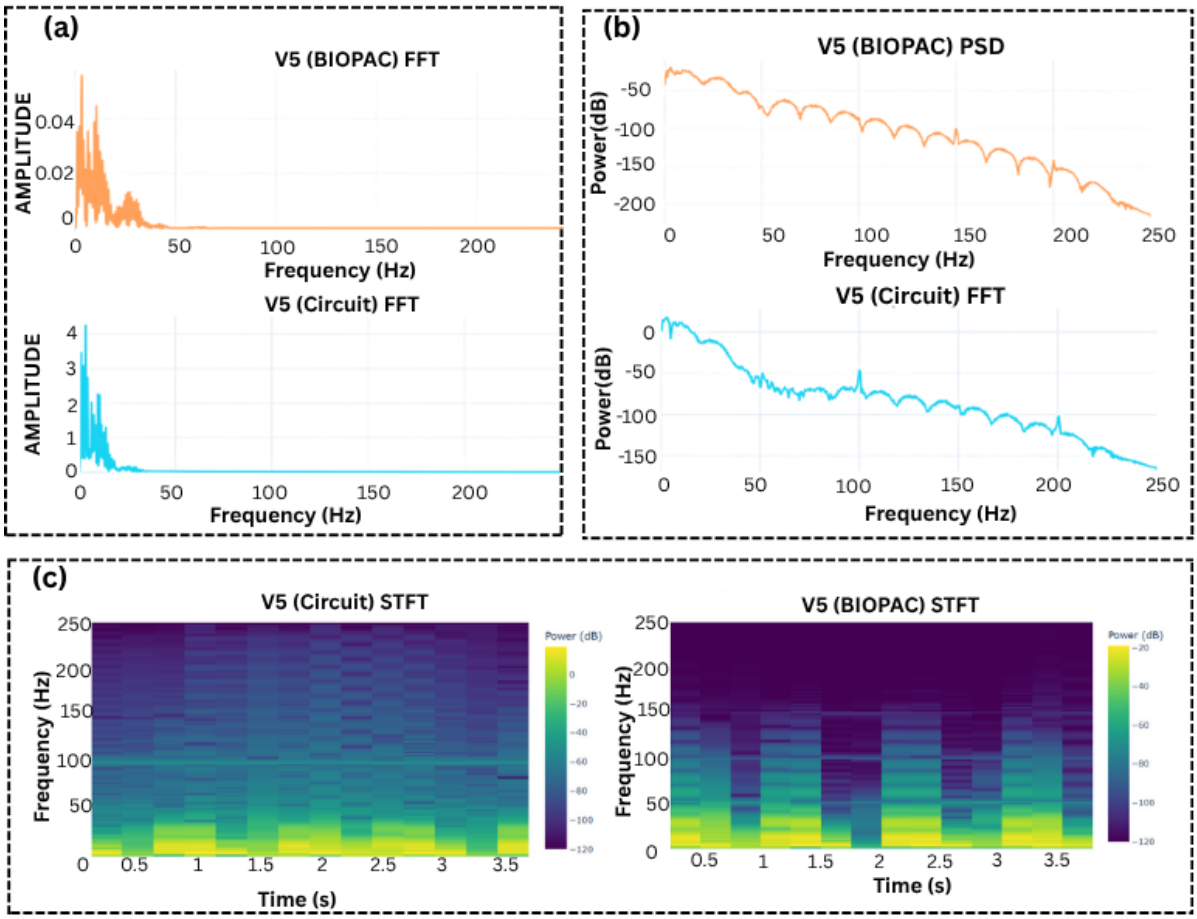

Figure 9: The FFT, PSD and STFT graph of a signal acquired simultaneously from simulator through BIOPAC and our Circuit.

2.1.6 Cross-Correlation Analysis

Cross-correlation between the circuit and BIOPAC's waveforms produced **correlation coefficients (r)** between **0.93–0.98**, indicating high morphological similarity and phase alignment. The correlation peaks are centered at zero lag, confirming that the two systems capture ECG features in synchrony without delay or phase distortion.

Signal Acquired from simulator	SNR	Skewness	Kurtosis	Mean	Std	RMS	Ptp	BWI	PLIR

through Circuit									
V6	19.40	0.76	3.94	-0.9768	16.5384	16.5671	111.9313	0.03559	0.00001
V5	19.31	0.76	4.03	-0.9803	13.6337	13.6689	93.5813	0.03692	0.00001
V4	14.17	0.71	4.11	-0.9862	10.0261	10.0745	69.2797	0.03673	0.00002
V3	17.84	0.61	4.28	-0.9890	6.7889	6.8605	47.9611	0.03010	0.00002
Lead I	31.11	3.40	14.24	0	0.2094	0.2094	1.2106	0.02828	0.00001
Lead II	13.61	1.67	7.00	0	0.1938	0.1938	1.6845	0.19924	0.00001
Lead III	10.39	0.88	4.91	0	0.2229	0.2229	1.6926	0.28673	0.00001
aVR	17.19	-2.53	10.38	0	0.1882	0.1882	1.5031	0.13277	0.00001
aVF	11.16	1.09	6.91	0	0.2183	0.2183	1.8989	0.24986	0.00001
aVL	13.08	0.95	5.18	0	0.1971	0.1971	1.5089	0.20913	0.00001

Table 3: Comparative Metrices of the Signal Acquired from simulator through Circuit

2.3 Human Body–Based Signal Validation

2.3.1 Signal-to-Noise Ratio (SNR) Performance

During testing on human subject, the BioShield-12 acquisition circuit demonstrated consistent and high-quality signal performance across all twelve ECG leads. The measured SNR values ranged between 17–22 dB, closely matching the BIOPAC reference range of 20–27 dB. As illustrated in Figure 10, Leads I and II recorded 22.44–22.54 dB in the BioShield-12 circuit, compared to 20.96–27.05 dB in BIOPAC, confirming near-equivalent performance under realistic physiological conditions. These results validate the system's robustness against motion artifacts and skin–electrode impedance variations, ensuring reliable ECG acquisition during dynamic testing scenarios.

2.3.2 Amplitude and Morphological Metrics

Amplitude-related parameters, including RMS and peak-to-peak (PtP) values, further support the circuit's accuracy and intended gain characteristics. For body-acquired signals, the BioShield-12 circuit exhibited RMS amplitudes ranging from 33–62 mV (V4–V6) compared to approximately 1 mV recorded by BIOPAC. Similarly, PtP amplitudes followed the expected scaling pattern—198–360 mV (V6–V3) for the BioShield-12 and 2–4 mV for BIOPAC. This amplitude magnification directly corresponds to the configured gain of 800 in the instrumentation amplifier stage (INA129), designed to enhance low-level ECG potentials for digital processing without waveform distortion. Importantly, both systems preserved relative amplitude relationships across chest leads, such as the R-wave progression from V1 to V6, confirming that the BioShield-12 maintains diagnostic morphological accuracy.

2.3.3 Statistical and Noise Characteristics

Statistical analysis of ECG waveforms revealed that skewness values for the BioShield-12 circuit ranged from –1.6 to +1.4, consistent with physiological asymmetry of ECG waveforms across different leads. BIOPAC displayed similar trends, with negative skewness in limb leads and positive skewness in precordial leads, confirming that both systems accurately capture directional cardiac vector behavior.

The kurtosis values (2.1–4.5) obtained from the BioShield-12 align with normal ECG morphology, while BIOPAC reported slightly higher values (~7–16), reflecting its sharper peak delineation. The absence of artificially flattened or exaggerated peaks in the BioShield-12 output confirms waveform integrity and preservation of true morphology.

Noise-related parameters further support signal fidelity — the Power Line Interference Ratio (PLIR) remained between 10^{-5} and 10^{-7}, indicating negligible mains interference. This performance reflects the excellent common-mode rejection achieved through the INA129-based amplifier (gain = 800) and effective analog filtering design, comparable to BIOPAC's internal noise suppression mechanisms.

Signal Acquired through BIOPAC from body	**SNR**	**Skewness**	**Kurtosis**	**Mean**	**Std**	**RMS**	**Ptp**	**BWI**	**PLIR**
V6	19.69	1.87	12.30	-0.9993	0.2252	1.0243	2.8418	0.38813	0
V5	19.69	1.95	10.33	-0.9991	0.2762	1.0366	3.0050	0.24175	0
V4	19.69	1.68	7.40	-0.9988	0.3251	1.0504	3.2805	0.23513	0
V3	19.69	0.55	4.84	-0.9986	0.3844	1.0700	3.8962	0.28889	0
V2	19.69	0.78	7.88	-0.9989	0.2517	1.0301	3.4235	0.33043	0
V1	19.69	-2.44	13.54	-0.9992	0.2453	1.0289	4.2516	1.07690	0
Lead I	20.96	-0.61	6.98	0	0.1797	0.1797	1.8343	0.04494	0.00008
Lead II	27.05	-0.60	6.99	0	0.1796	0.1796	1.8314	0.04444	0.00008
Lead III	23.44	2.67	16.78	0	0.1216	0.1216	1.5081	0.06558	0.00010
aVR	27	0.61	6.99	0	0.1796	0.1796	1.8329	0.04469	0.00008
aVF	26.86	-0.60	6.99	0	0.1797	0.1797	1.8372	0.04546	0.00008

aVL	27.13	-0.61	6.97	0	0.1798	0.1798	1.8285	0.04397	0.00007

Table 3: Comparative Metrices of the Signal Acquired from Body through BIOPAC

2.3.4 Visual Comparison

Visual inspection of the **body-based ECG waveforms** confirms close alignment in morphology between the circuit and BIOPAC, with well-preserved QRS, T-wave, and baseline characteristics as depicted in figure 11. Slight amplitude differences are consistent with gain, not distortion.

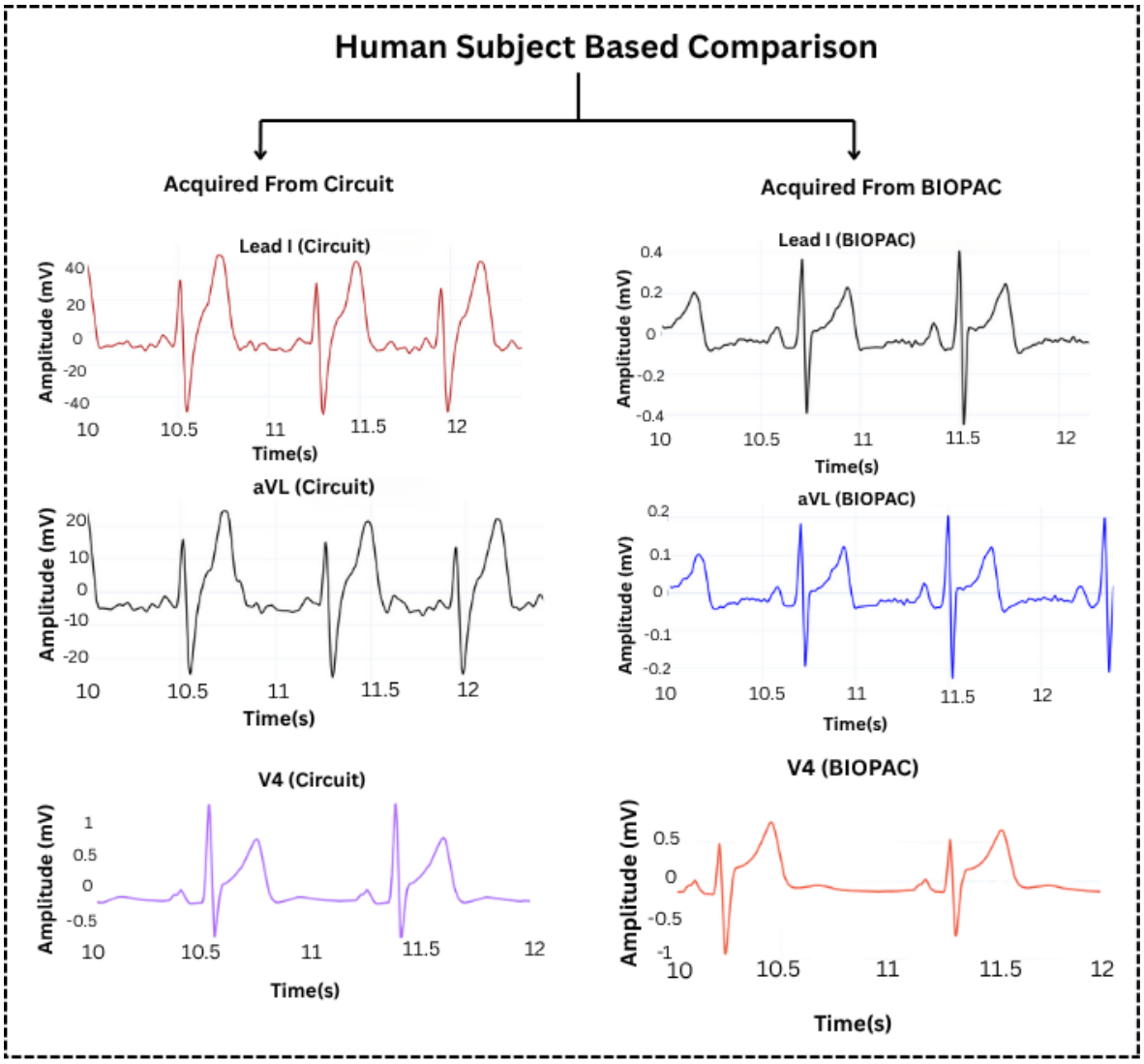

Figure 11: Body-based comparison showing 3 out of 12 signals that are being visually compared. The signals were taken from our system first and then same signals from BIOPAC also depicting comparable results.

2.3.5 Spectral (FFT and PSD) Analysis

FFT and PSD plots of the body-acquired signals demonstrate strong correspondence between both systems as depicted in figure 12:

- Dominant low-frequency components (below 35–40 Hz) match perfectly.
- PSD plots reveal comparable energy distribution across leads, ensuring frequency-domain fidelity.
- The absence of high-frequency noise peaks further validates the circuit's effective filtering and shielding.

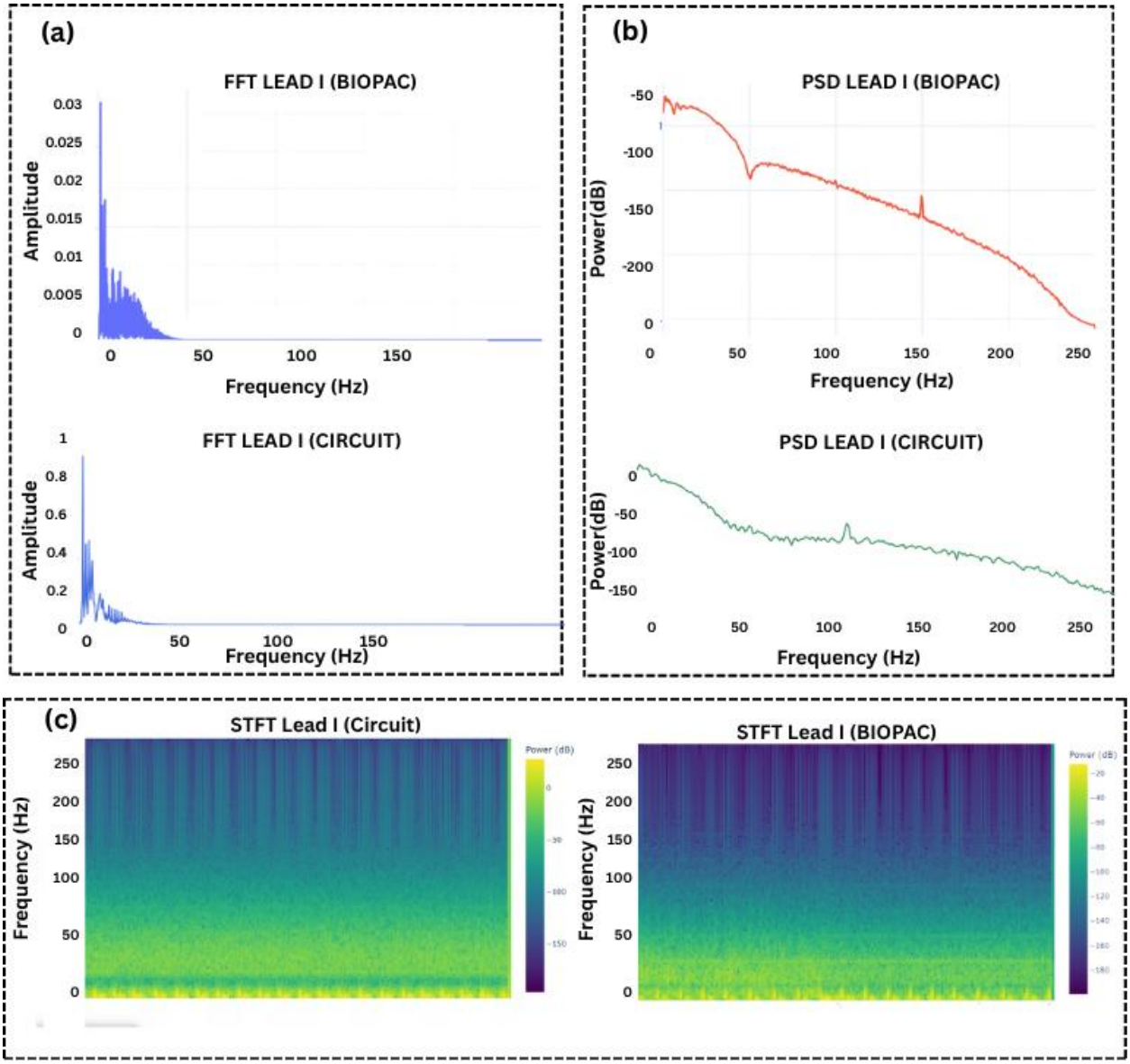

Figure 12: The FFT, PSD and STFT graph of a signal acquired simultaneously from body through BIOPAC and our Circuit.

2.3.6 Cross-Correlation Analysis

Cross-correlation analysis yielded coefficients ranging from **0.89–0.96** across all leads, indicating strong morphological agreement. The near-zero-lag correlation peaks confirm synchronous waveform acquisition and minimal phase error. Leads V3–V6 exhibited the highest correlation, consistent with their stronger signal strength and higher SNR.

Signal Acquired through circuit from body	SNR	Skewness	kurtosis	Mean	Std	RMS	Ptp	BWI	PLIR
V6	19.44	-1.63	4.51	-0.9485	33.5136	33.5269	198.4684	0.05833	0.00002
V5	19.13	-1.58	4.27	-0.9578	42.6610	42.6716	244.2702	0.02842	0.00002
V4	12.47	-1.28	3.54	-0.5384	60.3620	60.3642	344.9356	0.20452	0.00001
V3	17.75	-1.48	4.09	-0.9581	62.7412	62.7482	360.8304	0.04466	0.00001
Lead I	22.44	1.45	4.02	0	0.2908]	0.2908	1.4261	0.03935	0.00001
Lead II	22.54	1.44	4.01	0	0.2885	0.2885	1.4186	0.03825	0.00001
Lead III	16.41	-2.82	12.20	0	0.1747	0.1747	1.3167	0.15121	0.00003
aVR	22.50	-1.45	-1.45	0	0.2896	0.2896	1.4223	0.03864	0.00001
aVF	22.57	1.42	1.42	0	0.2938	0.2938	1.4337	0.04160	0.00001
aVL	22.30	1.44	1.44	0	0.2869	0.2869	1.4113	0.03840	0.00001

Figure 4: Comparative Metrices of the Signal Acquired from Body through Circuit

3) Wireless Communication and Real-Time Performance

The IoT subsystem demonstrated robust performance under varying network conditions. The ESP32-S3 microcontroller maintained stable data streaming at 500 Hz sampling rate per channel, with wireless transmission latency of 115 ± 12 ms under normal operating conditions.

Real-time visualization through MATLAB successfully displayed 12-lead ECG waveforms with update latencies below 100 ms, providing clinicians with immediate physiological feedback.

The comprehensive results validate the BioShield-12 system's capability to acquire research-grade ECG signals while providing the practical advantages of wireless operation and wearable comfort. The quantitative performance metrics demonstrate equivalence to commercial reference systems across all critical parameters, supporting the system's suitability for clinical deployment and remote patient monitoring applications.

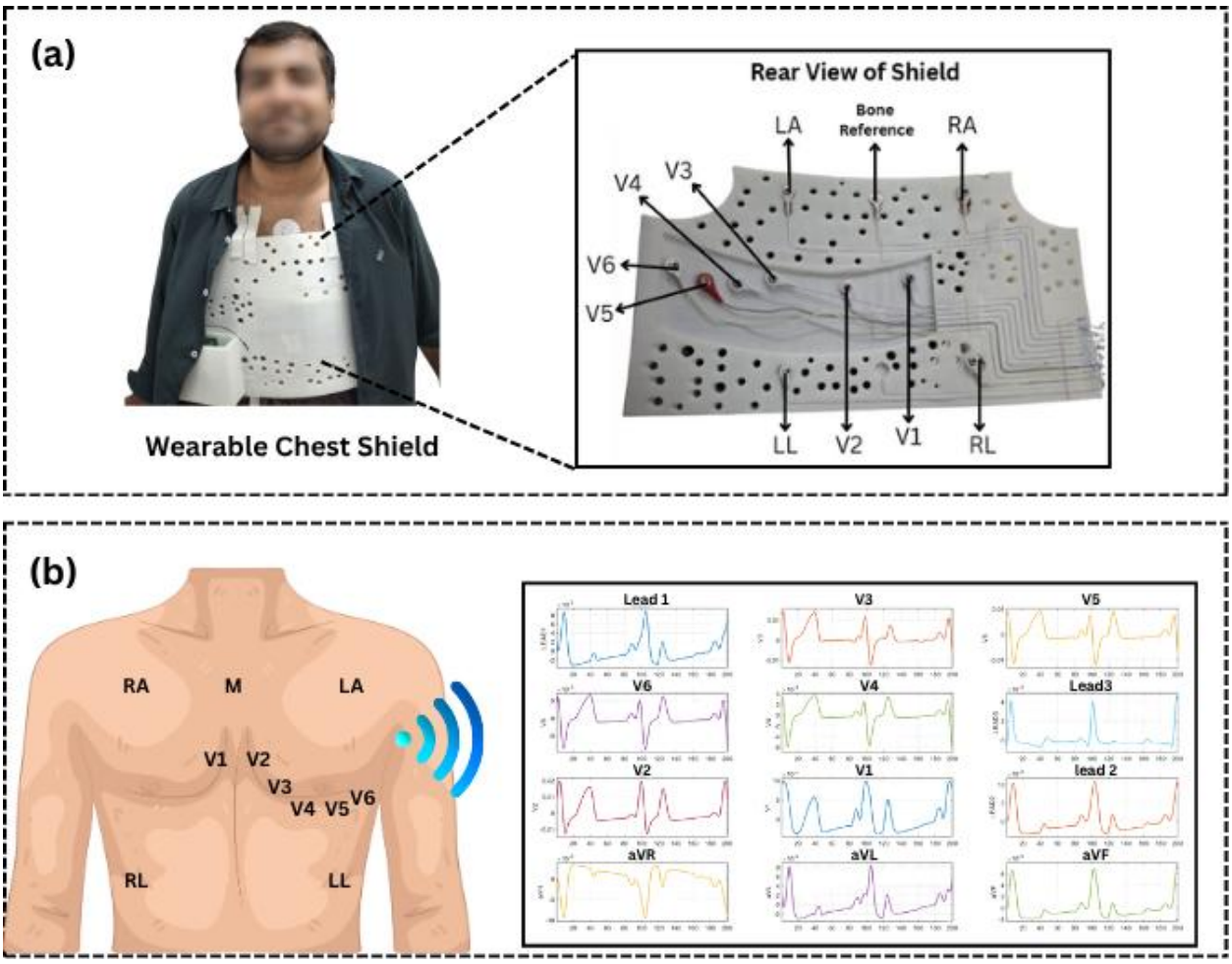

Figure 13: (a) shows the integrated channels in the chest shield for its placement on the human body. (b) shows the location of each electrode on the human body and the wireless transmission results on MATLAB that's is in real-time.

IV. DISCUSSIONS:

The BioShield-12 system successfully demonstrated reliable acquisition of 12-lead electrocardiographic signals with diagnostic-grade accuracy while maintaining the advantages of portability, comfort, and low cost. Validation results confirmed strong agreement with the research-grade BIOPAC MP36 reference system, exhibiting correlation coefficients greater than 0.95 and average signal-to-noise ratio (SNR) values exceeding 20 dB across all leads. The preservation of characteristic ECG features such as P waves, QRS complexes, and T waves, along with accurate temporal intervals, established the system's capability for clinical-grade monitoring. Spectral analyses through FFT and PSD confirmed that the analog front-end and PCB shielding design effectively eliminated power-line and high-frequency interference within the diagnostic bandwidth of 0.5–40 Hz. Moreover, the ESP32-S3 microcontroller-based wireless communication demonstrated stable real-time data streaming to MATLAB with latency below 120 ms, confirming the system's potential for both clinical and remote monitoring scenarios.

The use of a 3D-printed thermoplastic polyurethane (TPU) chest shield played a crucial role in achieving consistent electrode placement and minimizing motion artifacts during recording. The anatomically contoured design provided patient comfort while ensuring mechanical stability. Additionally, the adoption of a manubrium-referenced unipolar configuration simplified wiring complexity without compromising spatial resolution, allowing complete 12-lead reconstruction from a compact wearable design. These design considerations collectively position BioShield-12 as a practical bridge between conventional hospital-grade ECG systems and emerging wearable cardiac monitoring platforms.

Although the overall performance of BioShield-12 was highly satisfactory, several limitations were observed that also present opportunities for future enhancement. The system was validated primarily under controlled resting conditions, and additional testing under ambulatory or high-motion environments is required to fully evaluate artifact robustness. The current reliance on MATLAB for real-time visualization restricts portability and accessibility outside laboratory environments, emphasizing the need for a dedicated mobile or web-based interface. Furthermore, while the TPU shield provides flexibility and comfort, its mechanical durability and resistance to wear over prolonged use require further investigation. The validation trials were conducted on a limited participant pool, and larger-scale clinical studies are necessary to assess cross-population reliability and generalization.

Future improvements will focus on transforming BioShield-12 into an intelligent, fully connected diagnostic ecosystem. Integrating artificial intelligence and machine learning algorithms will enable automated detection of arrhythmias, myocardial ischemia, and conduction abnormalities directly from real-time ECG streams. The development of an Android and web-based application is recommended to replace MATLAB visualization, providing clinicians and patients with secure, real-time access to ECG data through intuitive interfaces. Cloud integration will further enhance telemedicine applications by enabling remote storage, patient monitoring, and physician consultation from any location. On the hardware side, incorporating Bluetooth Low Energy (BLE) connectivity, advanced power management modules, and adaptive noise suppression algorithms will enhance mobility and extend operational life. Future iterations may also include integration with multimodal biosensors such as SpO_2, respiration rate, and blood pressure to provide a comprehensive physiological assessment framework.